Proceedings of the International Conference on Oxide Materials for Electronic Engineering (OMEE 2021)

Development of Borate–Vanadate Glass Pure and Incorporated with La–Vanadate Nanoparticles

O. Chukova*, S.G. Nedilko and V. Scherbatskyi

Faculty of Physics, Taras Shevchenko National University of Kyiv, Volodymyrska Str., 64/13, 01601 Kyiv, Ukraine

Doi: 10.12693/APhysPolA.141.345 *e-mail: chukova@univ.kiev.ua

The concentration series of the lithium-vanadate-borate glass samples of $x\mathrm{Li_2O}$–$2\mathrm{V_2O_5}$–$(98-x)\mathrm{B_2O_3}$ (x = 8–58) composition was synthesized by the melt quenching procedure and studied. Some of the samples were doped with luminescent $\mathrm{LaVO_4}$:Eu,Ca vanadate nanoparticles. Emission spectra of the undoped samples consist of the wide bands of own luminescence peaked at 540, 650 and 720 nm, whereas spectra of the doped samples are linear and observed in the 570–720 nm spectral range. These spectra correspond to $\mathrm{Eu^{3+}}$ ions intrinsic emission. Lithium oxide component adding to the vanadate-borate glass composition increased the optical quality of the samples and affected their luminescence spectra. Manifestation of own luminescence together with the luminescence of the embedded $\mathrm{LaVO_4}$:Eu,Ca nanoparticles is a basis for the elaboration of glass-ceramics materials available for use as luminescent converters in WLEDs devices.

topics: luminescence, borate glass, vanadate, $\mathrm{Eu^{3+}}$

1. Introduction

Glass-ceramics (GCs), and in particular transparent glass-ceramics (TGCs), which consist of a glass matrix embedded with inorganic micro and nanosized crystalline particles (M/NPs), are solid state materials promising for various optical and optoelectronic applications [1–4]. Especially, they can be used as luminescent converter coverings for white light-emitting diodes (WLEDs). Formerly, some TGCs were elaborated on and studied with the aim to replace silicon-phosphor converters with phosphor-glass ones, but the researchers have mainly paid attention to luminescent YAG:Ce particles embedded into oxide glass matrices [1 , 5–7]. In many cases, multicomponent glasses (4–6 components) were used as matrices of glass-ceramics. Such glasses are used in order to reduce temperatures of the melting and processing of a glass. It is also important to take into account the interaction of the glass phase with crystalline particles. This interaction, especially at high processing temperatures, can significantly affect the properties of a manufactured glass-ceramic composite. (Particularly, it was difficult to avoid changing the M/NPs size under the effect of the relatively high temperature of their treatment). The use of multi-component glass was also associated with the efforts of researchers to conform refractive indexes of the glass matrix and crystal particles. Otherwise, the resulting glass-ceramic is often opaque or translucent, and it is characterized by strong light scattering.

It is easy to see that, in some cases, one of the components of the developed GCs was boron oxide $\mathrm{B_2O_3}$. It is not surprising because $\mathrm{B_2O_3}$ is one of the best glass-forming oxides. Materials based on the borate glass possess high mechanical, chemical and thermal stability, and they are widely used for the needs of optical science, related techniques, and biomedical applications [2, 8–10]. That is why, in our research on the development of glass-ceramic luminescent converters for WLEDs, we have focused on the borate glass matrix [11].

Our development has significant novelty compared to the above-mentioned works. (i) The vanadium oxide $\mathrm{V_2O_5}$, was added to the starting charge in the production of glass. It is known that $\mathrm{V_2O_5}$ modifies the structure of the borate glass network. This oxide can also be a glass-forming agent if its concentration is high [12–14]. (ii) Lanthanum vanadate nanoparticles doped with $\mathrm{Eu^{3+}}$ ions, $\mathrm{LaVO_4}$:Eu, were used by us as a crystalline component of glass-ceramics. The $\mathrm{LaVO_4}$:Eu luminescent properties have been studied by us in detail [15–17]. The presence of vanadate groups in the composition of both the glass matrix and the crystalline component can significantly increase the efficiency of glass-ceramics luminescence due to an increase in the light absorption from near-ultraviolet (UV) and violet (V) part of the visible spectrum [18–21]. These characteristics are very important for luminescent glass-ceramic converters, which are required for WLED devices. (iii) We also introduced alkali metal oxides, in particular lithium oxide $\mathrm{Li_2O}$, into

the borate glass matrix for the same purpose. It is known that the increase of alkali metal oxides content in the oxide glass leads to a shift of the optical absorption edge to longer wavelengths [22–25]. (iv) It should be noted that in WLEDs' covering materials, glass usually only plays a role of a binding media for luminescent particles incorporated there. In this work, we tried to point out that it is possible to find TGCs compositions in which the glass matrix emits its own luminescence in a wide visible spectral range. Borate glasses, which contain some vanadate groups, may just be such materials [15, 19, 26]. Own emission of the borate-vanadate glass matrix is a great advantage because it can improve color characteristics and enhance the effectiveness of the GCs luminescent converters for the WLED devices.

Thus, synthesis and study of concentration series of the "pure" lithium-borate-vanadate glasses $x\mathrm{Li_2O}$–$2\mathrm{V_2O_5}$–$(98-x)\mathrm{B_2O_3}$ (x = 8–58), as well as based on them glass-ceramics containing luminescent lanthanum vanadate particles is the goal of this work.

2. Experiment

The required calculated amounts of the boric acid $\mathrm{H_3BO_3}$, lithium carbonate $\mathrm{Li_2CO_3}$, and vanadium pentoxide $\mathrm{V_2O_5}$ (all of "chemically pure" qualification) were taken for the preparation of lithium–vanadate–borate glass samples. Recently, we have found that only the samples with 2–4 mass% of the vanadium oxide content are sufficiently transparent in the visible range and could be promising luminescent converters, while the vanadate-borate glass with higher content of vanadium oxide is characterized by brown color, that is not desirable for applications in WLEDs [11] (Fig. 1a). Thus, the vanadium pentoxide content of 2 mass% was selected for further research.

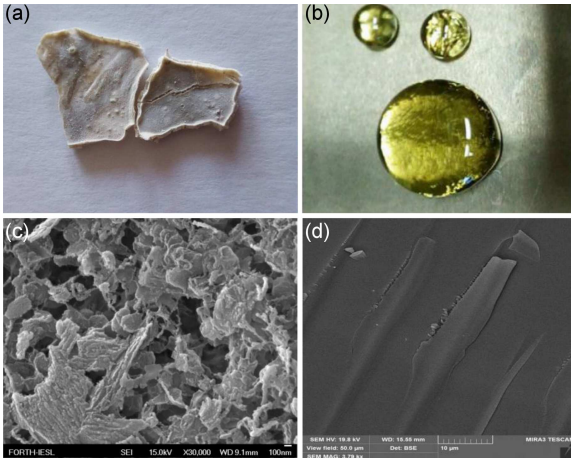

Fig. 1. Photo (a, b) and SEM images (c, d) of the $4\mathrm{V_2O_5}$–$97\mathrm{B_2O_3}$ (a, c) and $48\mathrm{Li_2O}$–$2\mathrm{V_2O_5}$–$50\mathrm{B_2O_3}$ samples (b, d).

The concentration of lithium component varied from 8 to 58 mass% with 10 mass% step. The reagents were ground, mixed, and placed in porcelain crucibles, then melted for 2 h in the air at 400°C and 4 h at 90°C in electric muffle furnace. After melting, the samples were quickly quenched using non-magnet metal plates. Some of the samples were embedded with the luminescent vanadate $\mathrm{La_{0.8}Eu_{0.1}Ca_{0.1}VO_4}$ nanoparticles synthesized by sol-gel method. Noted lanthanum vanadate composition was used as it showed maximal intensity of $\mathrm{Eu^{3+}}$ ions luminescence [15–17]. The compositions of the synthesized glass samples can be described by the general formula $x\mathrm{Li_2O}$–$2\mathrm{V_2O_5}$–$(98-x)\mathrm{B_2O_3}$, where x is the $\mathrm{Li_2O}$ content. The obtained samples were of good quality. All of them were transparent glass. The samples had a light coloring that gradually changed from light brown to yellowish, when the $\mathrm{Li_2O}$ concentration changed from 8 to 58 mass % (Fig. 1b).

SEM images of the samples were made for freshly chipped surfaces. Before SEM measurements, the surfaces were covered with thin metal films.

Luminescence spectra were measured using excitation with diode lasers (405, 478 and 532 nm) powerful Xenon lamp DXL-100 and registered using DFS-12 monochromator with grating 600 grooves/mm, slit on 50 μm and FEU-79 photomultiplier.

3. Results

The photoluminescence (PL) light of un-doped ("pure") glass visually was of yellow color. The emission was quite intensive when the PL was excited by laser radiation. Then thickened vivid yellow track from the exciting laser beam was clearly visible inside the glass. Figure 2a presents the PL spectra of the $x\mathrm{Li_2O}$–$2\mathrm{V_2O_5}$–$(98-x)\mathrm{B_2O_3}$ glass samples at λ_{ex} = 405 nm excitation. The PL spectra of the samples of low $\mathrm{Li_2O}$ content (Fig. 2a, curves 1, 2) are presented by the wide band in the range from 450 to 750 nm, covering almost the entire spectrum of visible light. The position of the emission band maximum is located near 540–570 nm at 405 nm excitation. Dependence of the maximum position and the long long-wave wing in spectra 1 and 2 in Fig. 2 is, obviously, a manifestations of the hidden PL bands. In fact, the PL spectra of the samples with higher $\mathrm{Li_2\hat{I}}$ content have been confirmed. There is a long-wavelength component with a maximum of around 700–720 nm in the spectra of these samples. The intensity of this PL component increases with $\mathrm{Li_2O}$ concentration increasing (Fig. 2a, curves 3, 4). At the same time, the relative intensity of the noted above short-wavelength spectral component decreases, and its maximum position shifts from 570 nm for x = 8 to 540 nm for x = 58. This change in the position may be the result of an increase in the intensity of a hidden PL component. If so, then we should assume that the maximum of the shortest wavelength band is near 540 nm.

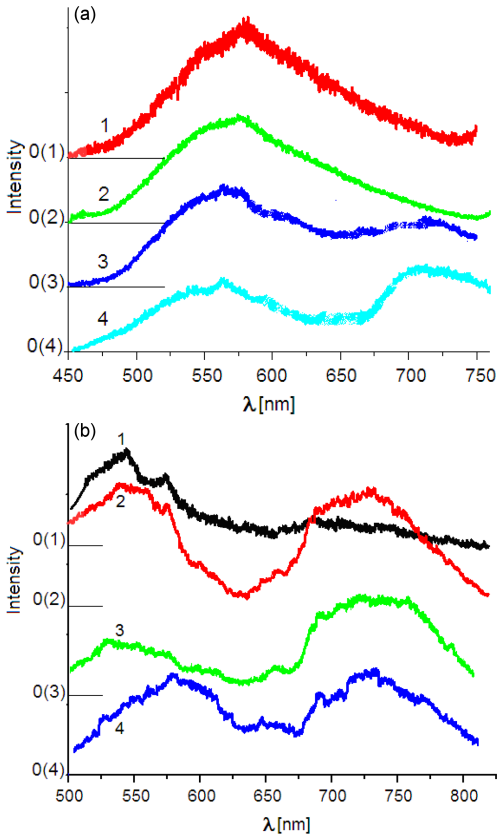

Fig. 2. Luminescence spectra of the $x$$Li_2O$–$2V_2O_5$–$(98 - x)B_2O_3$ glass samples. Here, x = 8 (1), 28 (2), 48 (3), and 58 (4); λ_{ex} = 405 (a) and 473 nm (b).

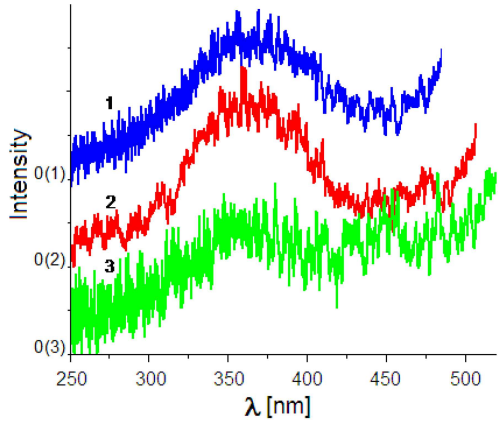

Fig. 3. Excitation spectra of the $48Li_2O$-$2V_2O_5$-$50B_2O_3$ sample at λ_{reg} = 550, 580 and 700 nm.

The PL spectra measured under excitations at λ_{ex} = 473 nm confirm made assumptions (Fig. 2b). These data, in general, are similar to those described earlier. However, the complex structure of the spectra was shown better there. It is clear that the contribution to the total spectra is given by three strongly overlapping components located in the ranges 500–620, 600–700 and 670–820 nm.

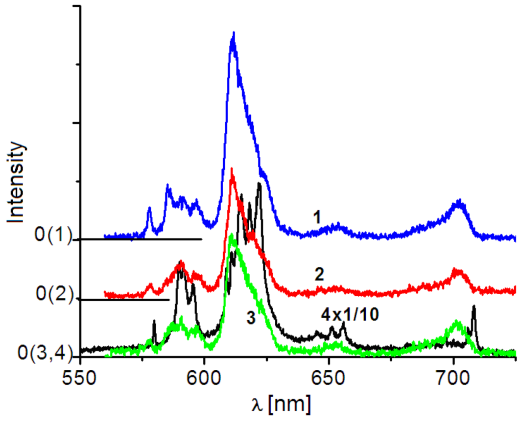

Fig. 4. Luminescence emission spectra of the $47Li_2O$–$2V_2O_5$–$50B_2O_3$–$1La_{0.8}Eu_{0.1}Ca_{0.1}VO_4$ GCs sample (1–3) and $La_{0.8}Eu_{0.1}Ca_{0.1}VO_4$ powder (4) at λ_{ex} = 532 (1), 473 (2) and 405 nm (3, 4).

Moreover, both the 500–620 and 670–820 nm regions obviously consist of at least two components each.

Luminescence excitation spectra registered at various areas of the PL spectra for the sample with Li_2O concentration x = 48 are presented in Fig. 3. They are broad band in the spectral range of 250–425 nm with a maximum of near 360 nm. The structure of the excitation spectra depends on the wavelength of the PL registration λ_{reg}, and therefore, we can also see a weak excitation component in the range 420–500 nm at λ_{reg} = 580 nm. This band becomes more noticeable for the PL registration at λ_{reg} = 700 nm (Fig. 3).

Luminescence spectra of the glass-ceramics samples of various compositions are shown in Figs. 4 and 5. The PL spectra of the $47Li_2O$–$2V_2O_5$-$50B_2O_3$–$1La_{0.8}Eu_{0.1}Ca_{0.1}VO_4$ glass-ceramics are presented in Fig. 4. The obtained spectra are observed in the range of 570–720 nm. They are linear and consist of four groups of lines at 570–580 (bands of lower intensity), 580–605, 605–635 (bands of the highest intensity), and 670–710 nm ranges. The maximum of emission is located at 611 nm. In the range of 570–605 nm, one can see a slight dependence in the distribution of intensities between individual lines depending on the wavelength of excitation light. In particular, there is an increase in the intensity of 577 and 585 nm lines at 532 nm excitation.

Luminescence spectra of the $17Li_2O$–$2V_2O_5$–$80B_2O_3$–$1La_{0.8}Eu_{0.1}Ca_{0.1}VO_4$ glass-ceramics sample were measured at the same ranges as for the previous sample. The PL spectra dependence on the excitation light wavelength for these samples is more noticeable, both for the lines 577 and 585 nm and for the range 605–635 nm, where a maximum intensity was manifested at 615 nm. These three peaks are indicated by arrows in Fig. 5.

4. Discussion

Although many publications have been devoted to description of the alkali-borate glasses luminescence, they mainly deal with luminescence of the ions of rear earth (RE) and transition (TE) elements or ions of heavy elements dopants [2, 9, 19, 24, 26]. Therefore, the interpretation of the observed wide band luminescence is a difficult task, as the PL properties of the $x\mathrm{Li_2O}$–$2\mathrm{V_2O_5}$–$(98-x)\mathrm{B_2O_3}$ composition were not described in the literature before. It is obvious that the vanadium oxide added to the glass is the main difference between the studied glass composition and the described elsewhere $\mathrm{Li_2O}$–$\mathrm{B_2O_3}$ alkali-borate glasses. Thus, it is logical to assume that vanadate groups or vanadium ions should be involved in luminescence processes in elaborated glasses. However, the physical nature of the observed emission cannot be reliably elucidated yet. Nevertheless, some considerations may be expressed. The similarity of the excitation spectra in Fig. 3 could indicate the similarity of the excitation processes of the various observed PL components. It should indeed be emphasized here that the observed PL excitation band and the excitations wavelengths applied by us (405 and 473 nm) lie on the edge of the vanadate-borate glasses absorption [18, 21, 22]. It means that two types of absorption (excitation) and luminescence scenarios can simultaneously occur in the studied systems. The first is the interband absorption caused by the main molecular groups that make up the vanadate-borate glass matrix. It is well known that those groups are mainly borate $(\mathrm{BO_4})^{4-}$ and $(\mathrm{BO_3})^{3-}$ anions [8, 12]. The vanadium dioxide, $\mathrm{V_2O_5}$, introduction to the glass is accompanied by vanadium ion transformation from $\mathrm{V^{5+}}$ to $\mathrm{V^{4+}}$ charge state in the form of the vanadyl ion ($\mathrm{VO^{2+}}$) of various coordination by oxygen ions in the glass matrix. It leads to a change in the local structure of glasses and promotes an increase of optical absorption in both the spectral range (250–500 nm), used by us for the PL excitation [18, 21, 22], and in longer wavelength range [21, 22, 26]. Then, excited energy transfer (EET) from borate anions to four coordinated $\mathrm{V^{5+}}$ ions ($\mathrm{VO_4^{3-}}$ molecular groups) as well as direct intra-molecular excitation of the noted vanadate groups leads to radiation transitions in the $\mathrm{VO_4^{3-}}$ groups [15, 26, 27] that cause the observed main bands of the PL. Some details of luminescence spectra can also be caused by radiation transitions in the vanadyl ions $\mathrm{VO^{2+}}$. Related bands in the PL spectra can be located near 420, 760–820 and 1000 nm [26].

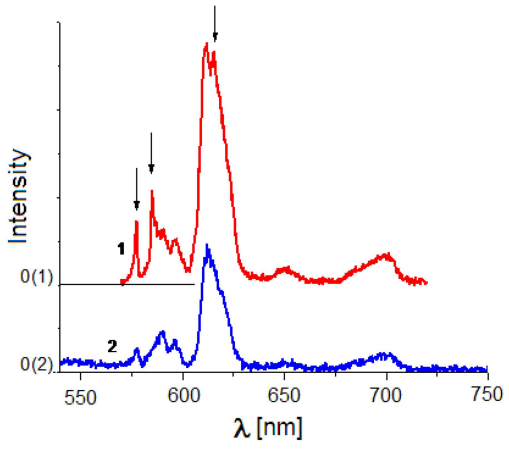

Fig. 5. Luminescence emission spectra of the $17\mathrm{Li_2O}$–$2\mathrm{V_2O_5}$–$80\mathrm{B_2O_3}$–$1\mathrm{La_{0.8}Eu_{0.1}Ca_{0.1}VO_4}$ sample at $\lambda_{ex} = 405$ and 532 nm.

Two types of oxygen vacancies, such as F (neutral) and F^+ electron deficient oxygen vacancy, always exist in large quantities in the oxide glass matrix, and they can originate in the PL bands with peak positions around 465 and 520 nm [26].

The second scenario of the PL process in studied glasses is recombination one, and it takes into account possible electron transition from the valence band (VB) to oxygen vacancy under excitation near the bottom of the conduction band (CB). (Average depth of the corresponding metastable states is about 0.2 eV below CB [28].) The formed holes are self-localized at the position of the bridging oxygen between the $(\mathrm{BO_4})^{4-}$ and $(\mathrm{BO_3})^{3-}$ groups of the glass matrix, thus forming a hole state with the energy level near 1.0 eV above the top of the VB [28]. So, radiation recombination of the thus formed electron-hole pairs can cause luminescence in the red range of the spectrum.

No doubt, various types of defects formed due to violations of the glass network structure or by uncontrolled impurities can exist in the manufactured glass. Obviously, if their concentration is very high, then the transfer of excitation energy or charge carriers to the before-mentioned PL centers is disturbed, and the luminescence of such glass may weaken. This situation, apparently, is realized for the glasses obtained with a vanadium dioxide content above 2 mass%. In fact, Fig. 2a and c showed that noted glasses are of low quality and characterized by significant violations of the structure. As a result, we were unable to register the luminescence of glasses of noted compositions.

However, we found that the addition of the lithium oxide improves the optical quality and structure of the glass (Fig. 2b and d), which apparently reduced non-radiation losses of excitation energy. Lithium oxide addition, as has been mentioned, influences the structure of the glass by changing the ratio of the number of $(\mathrm{BO_4})^{4-}$ and $(\mathrm{BO_3})^{3-}$ groups, and this change should lead to a change in the number of luminescence centers of different types and should be reflected in the optical properties. Actually, this is what we observed as the spectral changes in Fig. 2, depending on the oxide content.

The PL spectra of the glass incorporated with the $La_{0.8}Eu_{0.1}Ca_{0.1}VO_4$ NPs (spectra of the GCs samples) consist of linear components only (Figs. 4 and 5). The linear narrow bands observed in the emission spectra of these samples in the 570–580, 580–605, 605–635 and 670–710 nm spectral regions belong to the well-known $^5D_0 \rightarrow {}^7F_J$ (J = 0, 1, 2, 3, 4) electronic radiation transitions in the Eu^{3+} ions [15–17]. As the own emission of glass matrix was diminished for the case of GCs samples and Eu^{3+} ions were incorporated only into the crystalline particles, we can state that the effectiveness of the NP's luminescence excitation is higher compared to the glass. (The conditions of luminescence excitation were similar for both the glasses (see Figs. 1 and 5) and glass-ceramics (Figs. 4 and 5)). Besides, we have to suppose that EET occurs from glass to NPs. In fact, we see that the PL spectra of glass (Figs. 1 and 2) overlap with the Eu^{3+} ions absorption spectra [15–17]. Thus, the EET effect also promotes quenching the glass's own luminescence.

Other manifestations of interaction between glass matrix and embedded NPs were also found. In fact, redistribution of the relative intensity of the Eu^{3+} ions PL lines depending on the excitation wavelength (most noticeable changes are marked by arrows in Fig. 5) is related to the formation of two types of the Eu^{3+} PL centers of different site symmetry in NPs lattice. We have recently shown that noted two types of PL centers should be related to Eu^{3+} ions located inside and at the surface of the $LaVO_4$:Eu^{3+} NPs [15–17]. In this case, observed redistribution of intensity and shift of the positions of the lines in the PL spectra of NPs incorporated to the glass matrix compared to the spectra of Eu^{3+} ions emitting in the lattice of initial NPs nanoparticles (please, compare curves 3 and 4 in Fig. 4) confirm the impact of the glass environment on the Eu^{3+} ions located at the surface of NPs. Besides, it is easy to see that the fine structure of the Eu^{3+} ions PL spectra is weaker resolved in the case of NPs placed in the glass matrix (see Fig. 4, curves 3 and 4). This fact can be the manifestation of optical inhomogeneity lines broadening taking place for the Eu^{3+} ions located at the surface of NPs, where these ions are under effect simultaneously of the electric field of both NPs lattice and the glass matrix constituents.

5. Conclusions

The set of the lithium–vanadate–borate un-doped glasses (xLi_2O–$2V_2O_5$–$(98 - x)B_2O_3$, x = 8–58) was synthesized by melt quenching procedure and studied.

Increasing of lithium oxide content improves optical quality and modifies luminescence spectra of the vanadate–borate glass.

Glass-ceramics samples were made via doping noted glasses by the luminescent vanadate nanoparticles $LaVO_4$:Eu,Ca.

Manifestation of the own luminescence of the glass matrix and luminescence of the embedded $LaVO_4$:Eu,Ca nanoparticles under the same excitation wavelength creates a basis for the elaboration of glass-ceramics materials available for use as luminescent converters in WLEDs devices. However, further research is needed to increase the efficiency of wide band luminescence of the glass matrix.

Acknowledgments

This work has received funding from the Ministry of Education and Science of Ukraine within the Science in Universities Program and Bilateral Grants Program.

References

[1] D. Chen, W. Xiang, X. Liang, J. Zhong, H. Yu, M. Ding, H. Lu, Z. Ji, *J. Eur. Ceram. Soc.* **35**, 859 (2015).

[2] D. Ehrt, *IOP Conf. Ser. Mater. Sci. Eng* **2**, 012001 (2009).

[3] T.K. Yadav, A.K. Singh, K. Kumar, R.A. Yadav, *Opt. Mater.* **33**, 1732 (2011).

[4] P. Yongsiri, S. Eitssayeam, G. Rujijanagul, S. Sirisoonthorn, T. Tunkasiri, K. Pengpat, *Nanoscale Res. Lett.* **7**, 136 (2012).

[5] J. Wang, C.-C. Tsai, W.-C. Cheng, M.-H. Chen, C.-H. Chung, W.-H. Cheng, *IEEE J. Sel. Top. Quantum Electron.* **17**, 741 (2011).

[6] L. Wang, L. Mei, G. He, J. Li, L. Xu, *J. Am. Ceram. Soc.* **94**, 3800 (2011).

[7] L.-Y. Chen, W.-C. Cheng, C.-C. Tsai, J.-K. Chang, Y.-C. Huang, J.-C. Huang, W.-H. Cheng, *Opt. Express* **22**, A671 (2014).

[8] M. Bengisu, *J. Mater. Sci.* **51**, 2199 (2016).

[9] H. Lin, E. Y.-B. Pun, X. Wang, X. Liu, *J. Alloys Compd.* **390**, 197 (2005).

[10] R.R. Tummala, in: *Borate Glasses*, *Materials Science Research*, Vol. 12, Eds. L.D. Pye, V.D. Fréchette, N.J. Kreidl, Springer, Boston (MA) 1978, p. 617.

[11] T. Voitenko, O. Chukova, S.A. Nedilko, S.G. Nedilko, M. Androulidaki, A. Manousaki, E. Stratakis, in: *2020 IEEE 40th Int. Conf. on Electronics and Nanotechnology (EL NANO)*, 2020, p. 168.

[12] H. Rowson, *Inorganic Glass-Forming Systems*, Academic Press, London, New York 1967.

[13] B. Saddeek, M.S. Gaafar, *Bull. Mater. Sci.* **37**, 661 (2014).

[14] T. Nishida, S. Kubuki, K. Matsuda, Y. Otsuka, *Croat. Chem. Acta* **88**, 427 (2015).

[15] O.V. Chukova, S.G. Nedilko, A.A. Slepets, S.A. Nedilko, T.A. Voitenko, *Nanoscale Res. Lett.* **12**, 340 (2017).

[16] O. Chukova, S.A. Nedilko, S.G. Nedilko, A. Slepets, T. Voitenko, M. Androulidaki, A. Papadopoulos, E.I. Stratakis, *Springer Proc. Phys.* **221**, 211 (2019).

[17] O. Chukova, S.G. Nedilko, S.A. Nedilko, A.A. Slepets, T. Voitenko, *Phys. Status Solidi A* **215**, 1700894 (2018).

[18] C.A. Hogarth, A.A. Hosseini, *J. Mater. Sci.* **18**, 2697 (1983).

[19] P. Madhusudana Rao, M. Sugathri, *Int. J. Lumin. Appl.* **1**, 148 (2011).

[20] B. Peng, Z. Fan, X. Qiu, L. Jiang, G.H. Tang, H.D. Ford, W. Huang, *Adv. Mater.* **17**, 857 (2005).

[21] N. Laorodphan, P. Pooddee, P. Kidkhunthod, P. Kunthadee, W. Tapala, R. Puntharod, *J. Non. Cryst. Solids* **453**, 118 (2016).

[22] S.K. Arya, G. Kaur, K.J. Singh, *J. Non. Cryst. Solids* **432**, 393 (2016).

[23] Y.M. Lee, S.M. Hsu, S.W. Yung, T. Zhang, V.S. Huang, J.J. Wu, C.H. Hsu, T.S. Chin, *Mater. Chem. Phys.* **144**, 235 (2014).

[24] B.N.K. Reddy, B.D.R. Raju, K. Thyagarajan, R. Ramanaiah, Y.-D. Jho, B. S. Reddy, *Ceram. Int.* **43**, 8886 (2017).

[25] Y.B. Saddeek, *Physica B* **344**, 163 (2004).

[26] S.K. Arya, S.S. Danewalia, M. Arora, K. Singh, *J. Phys. Chem. B* **120**, 12168 (2016).

[27] T. Li, J. Luo, Z. Honda, T. Fukuda, N. Kamata, *Adv. Mater. Phys. Chem.* **2**, 173 (2012).

[28] W.M. Pontuschka, L.S. Kanashiro, L.C. Courrol, *Glass Phys. Chem.* **27**, 37 (2001).